RSC Advances

ROYAL SOCIETY OF CHEMISTRY

www.rsc.org/advances

RSC Advances

RSCPublishing

COMMUNICATION

PDMS membranes with tunable gas permeability for microfluidic applications†

Cite this: DOI: 10.1039/xoxxoooooox

A. Lamberti,[a*] S.L. Marasso,[a,b] M. Cocuzza[a,b,c]

Received ooth January 2012,
Accepted ooth January 2012

DOI: 10.1039/xoxxoooooox

www.rsc.org/

The air permeability of PDMS membranes is easily tuned acting on their composition. Varying the mixing ratio between oligomers and curing agent it is possible to strongly influence the chemical and mechanical properties of the elastomer resulting in a huge increase of the gas molecules permeation across the membrane.

PolyDiMethylSiloxane (PDMS) has become the preferred material for Lab On a Chip (LOC) and microfluidic analysis platforms due to its properties: easy processability, gas permeability, easy adhesion and bonding to different substrates, biocompatibility, transparency, low cost processing for device fabrication.[1-3] The PDMS permeability has extensively used to add new features and characteristics to microfluidic devices. Permeability has been employed to move fluids inside micro channels to obtain an accurate control of the liquid and a complete filling of the device.[4] Using this mechanism is then possible to fabricate pumps, valves or switching ports integrated directly on the chip avoiding any contamination of external material, since a thin membrane of PDMS acts as a barrier towards the reagents and biological species during handling. Microfluidic bioreactor systems take advantage of PDMS permeability to ensure gas diffusion inside the reaction chamber for cells culturing application.[5] In fact, gas permeation is essential for cells survival and evolution. Moreover, cells analysis needs long time experiments (from hours to days) and, usually, in an incubator at a fixed temperature of 37 °C.[6] This often involves bubbles arising inside the microfluidic channels and consequent potential test failure. In order to solve this issue PDMS permeability has been successfully exploited to appropriately remove bubbles inside microfluidics employing active debubbler.[7,8] Employing the same principle cells handling has successfully carried out.[4,9] Considered the wide range of applications of permeable PDMS membranes it is evident the great scientific interest in obtaining an easy and effective method to tune the PDMS permeability in a controlled way.

Previous investigations on the PDMS permeability were carried out focusing on the relationship between thickness, diffusion area and microchannels Aspect Ratio (AR) with respect to pressure.[10,11] In this work we propose a study on the material itself by varying the ratio between the oligomers and curing agent. In fact, while the influence of PDMS composition on the chemical properties and the mechanical behaviour is well known,[12-15] a characterization of the permeability properties with respect to composition is missing in literature. The experimental tests demonstrated that the composition is not a negligible parameter since flow rate variation up to 300 % was observed by increasing the mixing ratio (MR).

The high flexibility of the silicon-oxygen (Si-O) chains in silicones provides "openings", which are free volumes that allow gas diffusion inside the network.[16] Free volumes, often named "holes", thermally generates and disappears with the movement of polymer chains. The diffusion of gas molecules in the rubber membrane is a process in which the gas molecules migrate from "holes" to "holes". Figure 1a schematically depicts the three different mechanisms involved in permeation: the solution of the gas molecules at the polymer/gas interface, the diffusion through the membrane, and finally the evaporation out of the membrane. The rate of permeation is a specific function of a given gas and rubber and it depends on both solubility and the diffusion rate.

In most of applications, permeability of a membrane is used to characterize the rate of permeation. Permeability is usually calculated by the following equation[16]:

$$P = \frac{v*\delta}{A*t*(p_1-p_0)} \qquad (1)$$

Where, P is the permeability for a given gas in a given membrane, v is the volume of gas which penetrates through the membrane, δ is the thickness of membrane, A is the area of membrane, t is time, p1 is the partial pressure of the gas on the higher pressure side of the membrane, and po is the partial pressure of the gas on the lower pressure side of the membrane.

Before studying the permeability in microfluidic conditions we decided to investigate the chemical and mechanical properties of the PDMS membranes.

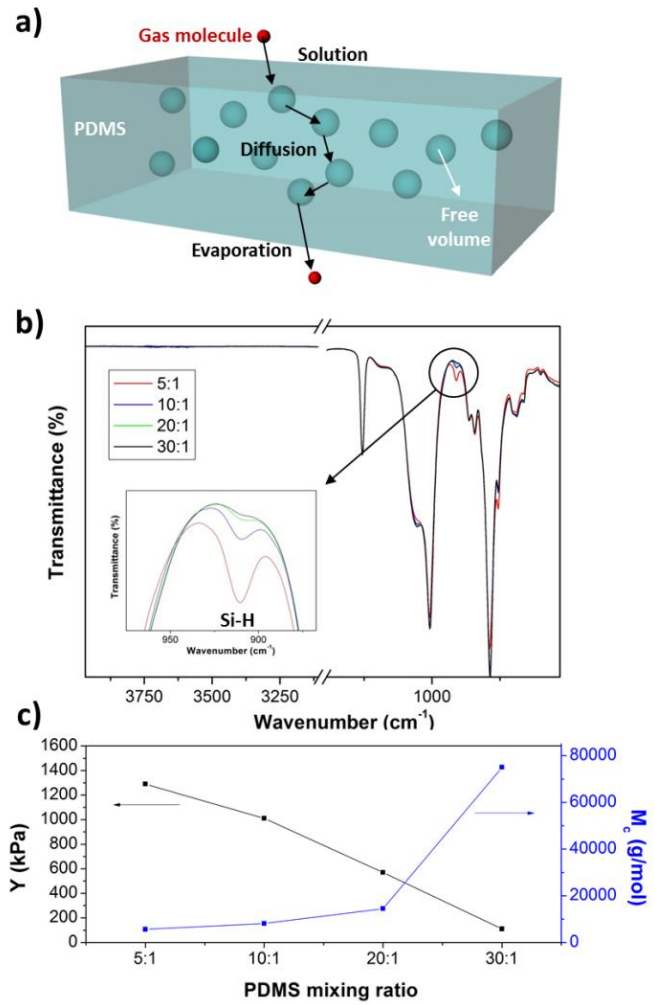

Figure 1. 3D scheme representing the gas diffusion mechanism in a PDMS membrane (a). ATR-FTIR transmittance spectra for PDMS at different mixing ratio (oligomer:crosslinker): 5:1, 10:1, 20:1, 30:1 (the inset shows the zoom of the Si-H vibrational band centred at 910 cm-1) (b).Young's modulus and cross-links value as a function of the mixing ratio (c)

PDMS samples for tensile measurements and IR characterization were prepared mixing the polymer base and the curing agent (Sylgard 184, Dow Corning) with different weight ratios (5:1, 10:1, 20:1 and 30:1). The mixture was then poured into PMMA moulds and thermally cross-linked (more details about the fabrication process can be find in the ESI).

Transmittance FTIR spectra, collected in Figure 1b, allow to analyse the influence of the MR between the PDMS oligomer and the curing agent on the resulting elastomeric network. The oligomer molecules are identified by the -Si(CH_3)$_2$O- repeating unit and vinyl termination groups (–CH=CH_2), while silicon hydride functionalities are characteristic groups of the curing agent.

The crosslinking reaction is described by the hydrosilylation of oligomer vinyl-terminations with the cross-linker Si-H groups. A MR equal to 10:1 is the standard composition (suggested by the producer) representing the correct balance between the two components in order to obtain the minimum amount of unreacted species in the cross-linked network. All the bands of the FTIR spectra can be assigned to PDMS group vibrational frequencies. The most pronounced intensity variation increasing the MR is associated with the silicon hydride group, which has a direct influence onto the resulting elastomeric network. The zoom reported as inset of Figure 1b allows to appreciate its behaviour: decreasing the amount of crosslink agent a gradually more slack lattice is obtained, which should correspond to a higher density of free volumes. Similar behaviour can be observed acting on the curing temperature as described by Berean and co-workers.[17] In their work they found that an optimal cross-linking temperature of 75 °C results in membranes with the highest gas permeation, significantly higher than those cross-linked at room temperature or above 100°C. This evidence was ascribed to the structure of polymer chains that form the highest intensity of Si-H stretching bonds resulting in a more relaxed polymer matrix. Thus the optimized structure and extra free volume increases the diffusion rate, allowing the gas molecules to move more easily within the polymer matrix at this optimum temperature.

Previous works[18,19] demonstrated that varying the mixing ratio of the bi-component elastomer precursors it is possible to strongly influence the mechanical properties of cross-linked material. For this reason the elastic modulus of the free-standing PDMS membrane was investigated by tensile measurements. The results collected in Figure 1c show that the Young's modulus increases with the amount of cross-linker since a tighter network is formed. Indeed lower than suggested quantities of crosslinker could lead to a lower crosslinking density.

The molecular weight between cross-links (*Mc*) was calculated by:

$$Mc = \frac{3\rho R_g T}{Y} \qquad (2)$$

where *Y* is the elastic modulus, R_g the gas constant and *T* the absolute temperature.[20]

The average molecular weight between cross-links (plotted together with *Y* in Figure 1c) resulted to be extremely high for the 30:1 mixing ratio where the quantity of prepolymer is in large excess with respect to the cross-linking agent and it decreased together with the ratio.

Looking at the tensile characterization, the 30:1 PDMS could be the best candidate in order to improve the gas permeability thanks to the high *Mc* and so supposedly higher free volumes between chains. Unfortunately the high disparity between prepolymer and curing agent leads to a highly sticky and not manageable PDMS film. For these reasons we discarded 30:1 PDMS for the flow rate analysis and we focused our attention on the remaining three compositions: 5:1, 10:1 and 20:1.

The three PDMS mixtures have been used to fabricate membranes by spin coating with thicknesses in the range 10-40 µm. After the thermal cross-linking, the area of the membrane was defined by manual cutting and peel off. The PDMS membrane was assembled following the experimental set up depicted in Figure 2a. 10:1 PDMS was used to replicate a microfluidic pattern designed for the permeability experiments (see ESI). The obtained microfluidic cover chip was manually assembled on top of a glass substrate exploiting the "stamp and stick" bonding.[21] The PDMS membrane was sandwiched between the outlet port of the channel and a homemade[11] PDMS interconnection exploiting the same bonding method as before (more details are reported in ESI).

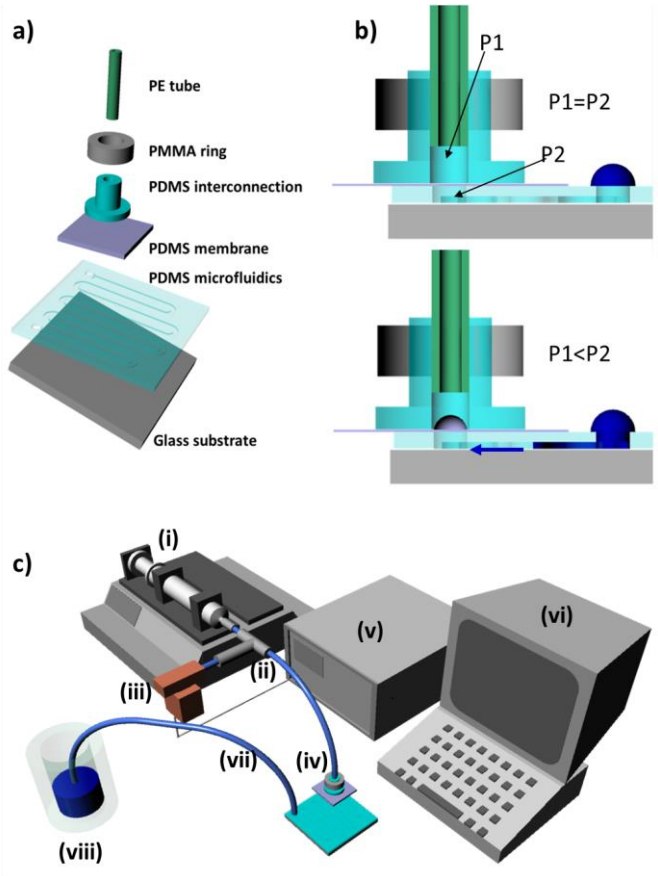

Figure 2. 3D scheme representing the assembling procedure of the microfluidic test device (a), cross-section images of the assembled structure in which the blue arrow indicates the flow direction (b), and the whole experimental set-up (c). The drop of blue dye in panel b) represents the liquid source while in panel c) the real tubing system experimentally used is shown (vii - viii).

The resulting device is a dead-ended microfluidic channel (Figure 2b). A suitably designed PMMA ring was used to avoid gas leakage when a polyethylene (PE) tube was connected to the PDMS interconnection (an in-deep description of microfluidic chip assembly is reported in the ESI). The fluidic characterization setup, depicted in Figure 2c, consisted on a syringe pump (i) connected through a 'T' joint (ii) to both a commercial pressure transducer (iii) and the PDMS interconnection (iv). Pressure data vs time were recorded through a multimeter unit (v) connected to a pc (vi). The pressure transducer was used in a feedback control circuit to maintain constant pressure with the syringe. The flow rate was measured by optical evaluation of the microchannel length filled by water under negative pressure (inset Figure 3). Knowing the section of the microchannel it is possible to calculate the air volume that has passed through the membrane in a certain time.

Flow rates across the PDMS membrane (20 μm thick) measured for various pressures are presented in Figure 3. The data exhibit a linear behavior in the range of applied pressure, but there is a noticeable difference among the three compositions. 10:1 PDMS behaves similarly to previously investigated membranes in analogous conditions.[4] Conversely the compositions that deviate from the standard MR show a totally different conduct.

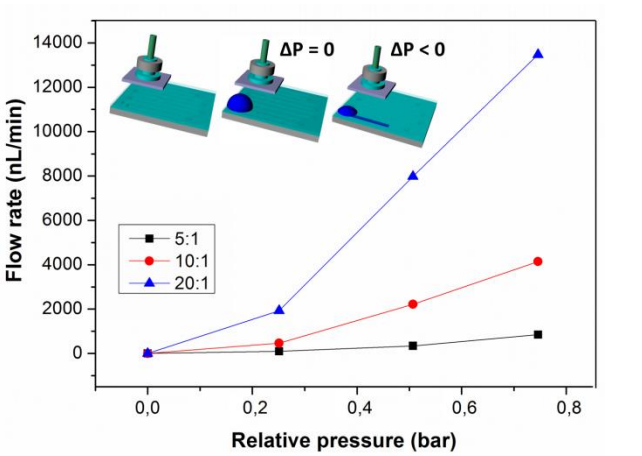

Figure 3. Air flow rate across PDMS membranes (20 μm thick) as a function of the relative pressure applied for the three PDMS compositions under investigation. The working principle of dead ended microfluidic channel for flow-rate measurements is represented in the inset.

As presupposed by mechanical measurements the 5:1 composition, with a very low molecular weight between cross-links, exhibits values of air flow-rate four times lower than the standard composition. On the contrary the 20:1 PDMS, characterized by the greater *Mc*, allows flow values up to 13000 nl/min.

In order to quantitatively evaluate the permeability values for the different PDMS compositions we need the real surface areas and thicknesses of the PDMS membranes when the gas pressure is applied. Indeed pressurized elastomeric membranes undergo a strain depending on their elastic modulus and a consequent thickness reduction. We have implemented a finite element model (by Comsol Multiphysics) representing the experimental setting with suitable boundary conditions to compute the desired values. The results are collected in Table S1 while a representative example of 3D maps obtainable by the structural-mechanical model is shown in Figure 4a. The maximum stress values are localized at the radial boundary of the membrane (clamped between the microfluidic channel and the top interconnection) and in the middle of the deflected area. Thanks to the calculated real areas and mean thicknesses of the pressurized PDMS membranes it is possible to evaluate *P* solving Eq1.

The resulting data are shown in Figure 4b and they exhibit a linear increase by reducing the amount of curing agent in the PDMS mixture. This trend is in line with the results of flow-rate measurements and with the assumption of higher free space density for increased MR. We find a linear pressure dependence of permeability coefficient for 5:1 and 10:1 PDMS composition. The sample 20:1 instead shows a decrease of the permeability for the higher pressure value investigated. This behavior can be explained considering that this composition exhibits the lowest elastic modulus and must therefore incur in the greater deformation of the membrane under pressure. The results of the simulation show that for 0.75 bar of pressure difference there is the greater percentage changes of area and thickness of the membrane. Recalling the dependence of the permeability (Eq. 1) by these two parameters it follows its decrease.

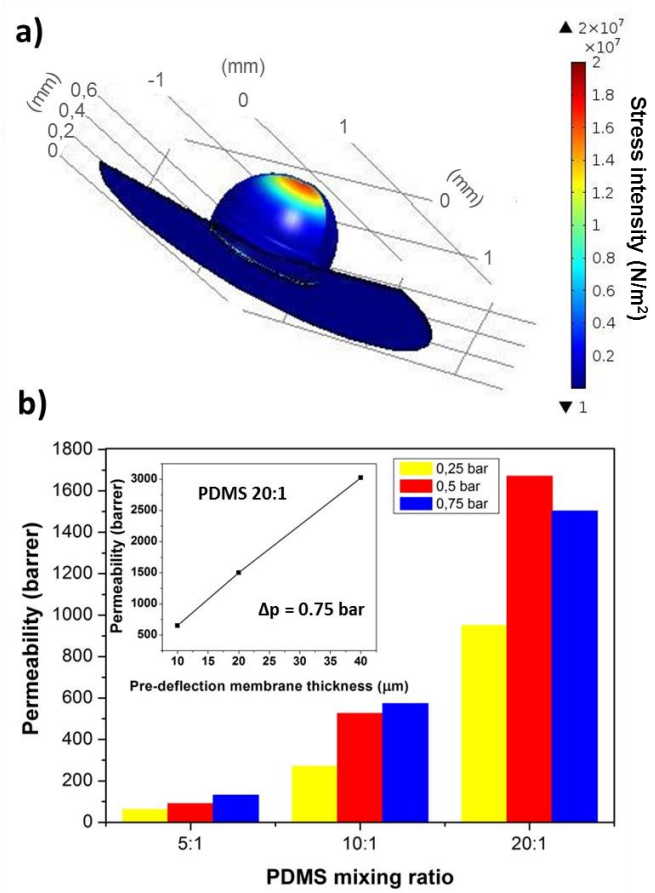

Figure 4. In a) an explicative FEM simulation result is reported: 3D map showing the deformation induced in the PDMS membrane (10:1, 20 μm thick) increasing the pressure while the stress intensity is graphically displayed as colour scale. In b) the comparison of PDMS membrane permeability varying the elastomer mixing ratio and the applied gas pressure is shown. In the inset the behaviour of PDMS permeability as a function of the pre-deflection membrane thickness is reported.

This dependence takes account that high pressure acting on the elastomeric sample can reduce the amount of free volume available for penetrant transport.[16] This effect should be much more evident as the polymer is deformable under stress.

With the aim to verify the dependence of PDMS permeability on the membrane thickness, three different thicknesses were fabricated and results are displayed as inset in Figure 4b.

As modelled by Equation 1, the permeability shows a linear relationship with membrane thickness and permeability increment of 500% is obtained passing from 10 to 40 μm thick samples.

Conclusions

In summary we have investigated the effect of PDMS composition on its permeation properties to air. The experimental set-up was designed in order to obtain information directly on the exploitability of PDMS membranes for microfluidic applications. The chemical and mechanical properties were investigated to gain a whole understanding on the material. FEM simulations were used to estimate the geometrical characteristics of the stressed membranes allowing the evaluation of permeability coefficients. Our work demonstrates that increasing the PDMS mixing ratio it is possible to boost the air permeability up to 300% with respect to the standard 10:1 composition. This result can be used to optimize the microfluidic devices in which the permeability of PDMS is the fundamental property simply acting on the precursors mixing ratio.

Acknowledgements

Authors would like to thank Dr. A. Chiappone for the help in tensile measurements, Dr. A. Ricci for the FEM simulations and Mr. J. Philippe for PDMS membrane preparation. This research has received funding from the Italian FIRB 2011 NEWTON (RBAP11BYNP).

Notes and references

[a] Department of Applied Science and Technology - DISAT, Politecnico di Torino, C.so Duca degli Abruzzi 24, 10129 Torino, Italy
[b] CNR-IMEM, Parco Area delle Scienze, 37a, 43124 Parma, Italy
[c] Center for Space Human Robotics @PoliTo, Istituto Italiano di Tecnologia (IIT), Corso Trento 21, 10129 Torino, Italy
* Corresponding author (A. Lamberti). Tel.: +39 011 090 7394; Fax: +39 011 090 7399; e-mail: andrea.lamberti@polito.it
† Electronic Supplementary Information (ESI) available. See DOI: 10.1039/c000000x/

1 S. K. Sia and G. M. Whitesides, *Electrophoresis*, 2003, **24**, 3563.
2 T. Fujii, *Microelec. Eng.*, 2002, **61–62**, 907.
3 J. Kuncová, P. J. & Kallio, *Eng Med Biol Soc Ann*, 2006, **1**, 2486.
4 M. A. Eddings, B. K. Gale, *J. Micromech. Microeng.*, 2006, **16**, 2396
5 E. Leclerc, Y. Sakai, T. Fujii. Biotechnology progress, 2004, **20**, 750.
6 E. Leclerc, Y. Sakai, T. Fujii, *Biomed. Microdev.*,2003, **1**, 109.
7 W. Zheng, Z. Wang, W. Zhang, X. Jiang, *Lab Chip*, 2010, **10**, 2906.
8 A. M. Skelley, J. Voldman, *Lab Chip*, 2008, **8**, 1733.
9 D. Irimia, M. Toner, *Lab Chip*, 2006, **6**, 345.
10 M. Johnson, G. Liddiard, M. Eddings, B. Gale, *J. Micromech. Microeng.*, 2009, **19**, 9
11 M. Quaglio, G. Canavese, E. Giuri, S.L. Marasso, D. Perrone, M. Cocuzza, C.F. Pirri, *J. Micromech. Microeng.*,2008, **18**, 10.
12 J. C. Lötters, W. Olthuis, P. H. Veltink, P. Bergveld, *J. Micromech. Microeng.*, 1999, **7**, 145.
13 A. Lamberti, M. Quaglio, A. Sacco, M. Cocuzza, C.F. Pirri, *Applied Surface Science*, 2012, **258**, 9427.
14 L. Pasquardini, C. Potrich, M. Quaglio, A. Lamberti, S. Guastella, L. Lunelli, M. Cocuzza, L. Vanzetti, C.F. Pirri, C. Pederzolli, *Lab Chip*, 2011, **11** 4029.
15 A. Lamberti, M. Di Donato, A. Chiappone, F. Giorgis, G. Canavese. *Smart Materials and Structures*, 2014, **23**, 105001.
16 T. C. Merkel, V. I. Bondar, K. Nagai, B. D. Freeman, I. Pinnau, *J Appl Polym Sci*, 2000, **38**, 415.
17 K. Berean, J. Z. Ou, M. Nour, K. Latham, C. McSweeney, D. Paull, A. Halim, S. Kentish, C. M. Doherty, A. J. Hill, K.

Kalantar-zadeh. Separation and Purification Technology, 2014, **122**, 96.

18 F. Carrillo, S. Gupta, M. Balooch, S. J. Marshall, G. W. Marshall, L. Pruitt, C. M. Puttlitz, *J. Mater. Res.*, 2005, **20** 2820.

19 A. I. Teixeira, S. Ilkhanizadeh, J.A. Wigenius, J.K. Duckworth, O. Inganäs, O. Hermanson, *Biomaterials*, 2009, **30** 4567.

20 N. Stafie, D. F. Stamatialis. M Wessling, *Sep. Purify. Technol.*, 2005, **45**, 220.

21 S. Satyanarayana, R. N. Karnik, A. Majumdar. *J. Microelectromech. S.*, 2005, **14**, 392.